Acta Chim. Slov. **2013**, *60*, (2), 343–350

343

Preparation, Characterization and Gas Permeation Investigation of Resorcinol-Formaldehyde Polymer or Carbon Xerogels/Tubular Ceramic Composites

Liviu Cosmin Cotet,[1,*] Kelly Briceño,[2] Carmen Ioana Fort,[1] Virginia Danciu,[1] Ricard Garcia-Valls[2] and Daniel Montané[3]

[1] *"Babes-Bolyai" University, Faculty of Chemistry and Chemical Engineering, Arany Janos st., 11, Cluj-Napoca, RO-400028, Romania*

[2] *Rovira i Virgili University, Department of Chemical Engineering, Av. Païssos Catalans, 26, Campus Sescelades, 43007, Tarragona, Spain*

[3] *Catalonia Institute for Energy Research (IREC), Bioenergy and Biofuels Division, Av. Països Catalans, 16, Campus Sescelades, 43007, Tarragona, Spain*

* Corresponding author: E-mail: ccosmin@chem.ubbcluj.ro

Received: 25-01-2013

Abstract

New very stable composites prepared by deposition of resorcinol-formaldehyde polymer (RF-) or carbon (C-) xerogels into walls of commercial porous tubular ceramics (TiO_2-ZrO_2 and αAl_2O_3-γAl_2O_3) were obtained by a sol-gel process followed by a drying and a pyrolytic (only for C-xerogel/ceramic composites) step. They were characterized by nitrogen adsorption-desorption, SEM and XRD, and tested for gas (H_2, CH_4, CO_2 and CO) separation applications. Additional morpho-structural information about the open-interconnected ultramicropore structure of composites was found by gas permeation investigation. Interesting results for H_2 permeance was obtained especially for RF-polymer/ceramic composites respecting Knudsen diffusion mechanism of gas permeance: $H_2 > CH_4 > CO > CO_2$. The coexistence of Knudsen and surface diffusion mechanisms were confirmed.

Keywords: Composite materials, xerogel, sol-gel process, porous ceramics, gas permeation

1. Introduction

In order to sustain the technological development in the fields of environmental protection[1] and energy production,[2,3] new material composites with suitable properties are required. One chapter of these fields is molecular sieve construction with application in fuel cell[2] and gas separation.[4] The main problems of molecular sieve manufacturing are the difficulties related to poor reproducibility and crack formation.[5,6]

Different studies have shown that polymeric and carbon membranes successfully compete in terms of stability, reproducibility and efficiency in gas separation comparing with other porous inorganic membranes, such as silica- and zeolite-based membranes which present complex and expensive fabrication ways.[4–10] The carbon materials not only have the ability to per-

form as molecular sieving but also may allow a considerably higher flux of the penetrant gases through the material as compared to zeolites with similar selectivity properties.[11] Also, the combination between polymeric or carbon porous materials with porous tubular ceramic supports provides very stable composite materials with higher potential for gas purification applications.[5,6,9,10]

Carbon molecular sieves based on novolac phenol–formaldehyde resin composites[12–15] and the gas diffusion properties of the carbon aerogel,[16,17] were evidenced. Both of these materials could be considered as akin materials of polymeric and carbon xerogels and are proper for composite material construction.[13–18] The most important characteristic of these material classes is the morpho-structural controllability of their nanoscale properties by the synthesis process.[16,17,19–23]

In this research, resorcinol-formaldehyde polymer (RF-) and carbon (C-) xerogels, obtained by sol-gel process, ambient drying followed by pyrolysis, were used as reinforcement part of composite membranes. Also, this part of the composite is considerate to be the active part in gas separation. As composite matrix, two commercial TiO$_2$-ZrO$_2$ and αAl$_2$O$_3$-γAl$_2$O$_3$ porous tubular ceramic with appropriate mechanical properties were used. These ceramics are successfully applied both as fluid separation membranes and as supports for other molecular membranes.[10,13,24]

The morpho-structural characteristics of obtained material composites were investigated by scanning electron microscopy (SEM), nitrogen adsorption and X-ray diffraction (XRD). Addition information about the pore features was revealed by gas permeation investigation.

Single gas permeances for pure interest gases (H$_2$, CH$_4$, CO$_2$ and CO), through prepared composite membranes at various trans-membrane pressures and room temperature, were determined. The unmodified ceramic supports and the corresponding RF-polymer or carbon aerogels[20]/ceramic composites were also tested in gas permeation. The results evidenced that due to their meso-macroporosity these are not proper for gas separation application.

2. Experimental

2. 1. Material and Reagents

Two types of support materials, TiO$_2$-ZrO$_2$ and αAl$_2$O$_3$-γAl$_2$O$_3$, were used to fabricate the composite membranes. The TiO$_2$-ZrO$_2$ monochannel tube ceramic support (**TAMI Industries**) had the outer radius of 10 mm and tube wall thickness of 2.4 mm. The tube wall presented external TiO$_2$ layer pore size distribution of 5 μm and thin internal ZrO$_2$ layer of 3 nm. The αAl$_2$O$_3$-γAl$_2$O$_3$ monochannel tube ceramic support (**Inopor**) had the outer radius of 10 mm and tube wall thickness of 1.4 mm. The pore size distribution of γAl$_2$O$_3$ external thin was 5 nm and αAl$_2$O$_3$ internal one was 3 μm.

Resorcinol (C$_6$H$_6$O$_2$, 98%, R), formaldehyde (CH$_2$O, 36.5%, F), Na$_2$CO$_3$ (99.9%, C), all from Aldrich, were used without further purification. Milli-Q purified water (W) was employed as solvent in all the experiments.

2. 2. Composite Preparation

Resorcinol (0.29 M) was dissolved in Milli-Q water under continuously stirring (R/W = 0.2 g cm^{-3}). Formaldehyde solution was added to the resorcinol solution (R/F = 0.5) under vigorous stirring. Afterwards, Na$_2$CO$_3$ aqueous solution 0.1 M was added to the previous mixture as polycondensation catalyst (R/C = 500).[20] After 10 min, the porous tubular ceramic supports were placed in the resulted solution and easily stirred to remove the pore air. Then, the glass vessel with the solution and ceramics were tight-

ly closed and cured: 1 day at room temperature, 4 days at 70 °C. The resulting resorcinol-formaldehyde (RF) wet gel deposited into ceramic walls were washed with acetone and dried in ambient conditions (1 atm, 25 °C). RF-xerogel deposited into ceramic walls resulted. The excess of RF-xerogel both from outside and inside of the ceramic tubes was removed. Only the RF-xerogel from inside of ceramic walls was kept. The obtained RF-xerogel/ceramic composite were pyrolysed at 750 °C for 2 hours in Ar atmosphere C-xerogel/ceramic composite resulting.

2. 3. Morpho-structural Investigation

SEM images were obtained with SEM-Quanta 200F.

Specific surface area, pore size distributions, and pore volume were determined with Sorptomatic SO-1990 device by using Brunauer–Emmett–Teller (BET), Barrett–Joyner–Halenda (BJH) and Horvath-Kawazoe (HK) calculation methods. Before measurements the samples were degassed at 120 °C for about 12 h.

XRD patterns were recorded in θ–2θ Bragg-Brentano geometry with Siemens D5000 powder diffractometer having Cu-Kα incident radiation (λ = 1.5406 Å).

2. 4. Permeation Measurement

The RF- or C-xerogel/tubular ceramic membranes were placed in a stainless steel module and sealed with Viton o-rings to perform the gas permeation experiments.[5,6] This reactor-module presented two input ways, for the feed of interest gases and carrier gas respectively, and two outputs, one for membrane uncrossed gas and the other one for membrane crossed and carrier gas mixture. Also, the module presents a tubular shape with 7.2 cm length, an inner diameter of 1.10 cm and an external diameter of 3 cm. The rout of interest gas through membrane wall came from outside to inside of tubular ceramic where was taken by the carrier gas to a mass spectrometer (Pfeiffer Vacuum Technology).[6]

Mass flow controllers were from Bronkhorst (0 – 100 mL min^{-1}). Pure H$_2$, CH$_4$, CO$_2$, CO and Ar, supplied from Air-Liquid Company were used to feed the membrane. H$_2$ was considered the main interest gas and Ar was used as carrier gas.

In order to build the calibration curves the gas (H$_2$, CH$_4$, CO$_2$, or CO) was mixed with Ar (10 – 100 : 10 and 10 – 100 : 50 ratios) in by-pass mode of the reactor measurement way. Normal operation permeance measurements were done at room temperature and 1 – 3 bar pressure difference.

3. Results and Discussion

Using suitable R/C and R/W sol-gel synthesis parameters a wet RF-gel with low shrinkage and small pore diameter after environmental drying and pyrolytic steps

Acta Chim. Slov. **2013**, *60*, (2), 343–350

345

we aimed. It was observed that the presence of TiO_2-ZrO_2 and αAl_2O_3-γAl_2O_3 ceramics inside of the started sol-gel solution decreased the gelation time. Thus, ceramics could be considered as additional catalysts, besides Na_2CO_3, for polycondensation reaction of resorcinol and formaldehyde. After the gel excess removal from the outside of the wall, tubular RF- or C-xerogel/ceramic composites without loss of xerogel from inside of ceramic walls were obtained.

The mass increasing reported to the Blank-ceramics was 8.6% and 2.7% for RF-xerogel/TiO_2-ZrO_2 and RF-xerogel/αAl_2O_3-γAl_2O_3, respectively. In the case of C-xerogel/TiO_2-ZrO_2 and C-xerogel/αAl_2O_3-γAl_2O_3, due to mass lost during the pyrolysis process, only a mass increasing of 3.2% and 1.85%, respectively was observed.

3. 1. Morpho-structural Characterization

Used αAl_2O_3-γAl_2O_3 (Figure 1) or TiO_2-ZrO_2 (Figure 2) were investigated by SEM both as blank ceramics (a) and as composites modified with RF-xerogel (b) or C-xerogel (c). The polymeric (Figures 1b, 2b) and carbon xerogel (Figures 1c, 2c) structures filling the whole space of the macro-mesoporous structure of the ceramic walls were

re visualized. After the pyrolytic step an increase of roughness of the resulted C-xerogel is evidenced.

By N_2 adsorption-desorption investigation, isotherms with thin loops specified for micro-mesopore structure were observed for RF- and C-xerogel/ceramic composites (Figure 3a). A strong difference between xerogel/ceramic composites and RF-xerogel collected from outside of the membrane composite walls (Exs-RF-xerogel) were evidenced by BET, BJH and HK methods (Figure 3b, Table 1). The Exs-RF-xerogels present higher surface area (~a 320 m^2 g^{-1}), cumulative pore volume and cumulative pore area, and multimodal mesopore size distribution. The obtained xerogel/ceramic composites present very low surface area (< 5 m^2 g^{-1}) and pore volume (< 0.015 cm^3 g^{-1}) determined by HK method, which are unspecific characteristics of the micro-mesoporous materials and is based on a slit-shaped pore assumption.[25]

According to F. Rouquerol et al. in the case of pore no greater than a few molecular diameters (d < 0.7 nm, ultramicropore), the N_2 pore filling occurs at a very low p/p^o (*i.e.* < 0.01).[25] E. Maglara et al. have revealed by high-resolution studies that the filling of ultramicropores is expected to occur at $p/p^o < 10^{-5}$.[26] Once the micropores have been filled, the plots become linear proving that capillary
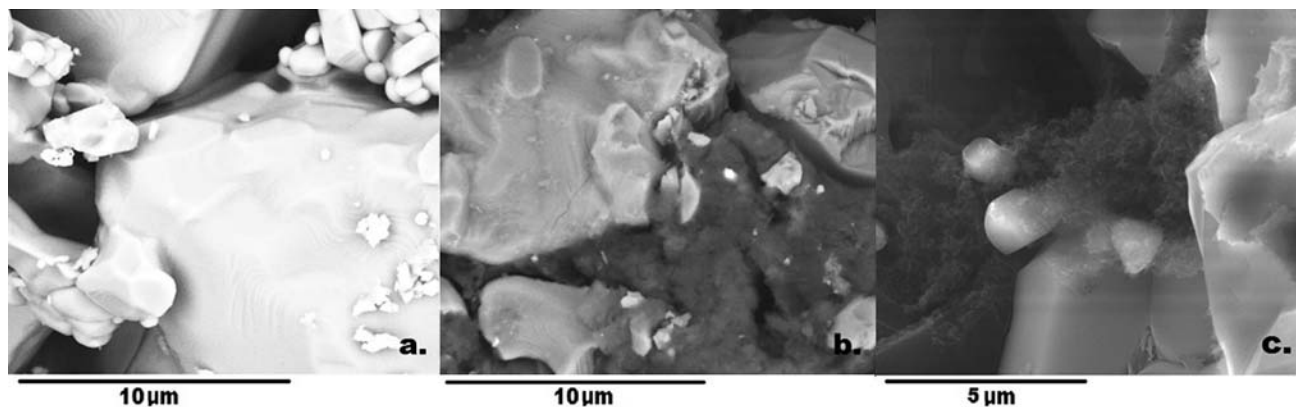

Figure 1. SEM imagines of αAl_2O_3-γAl_2O_3 tubular ceramic (a), RF-xerogel/αAl_2O_3-γAl_2O_3 (b), and C-xerogel/αAl_2O_3-γAl_2O_3 (c).
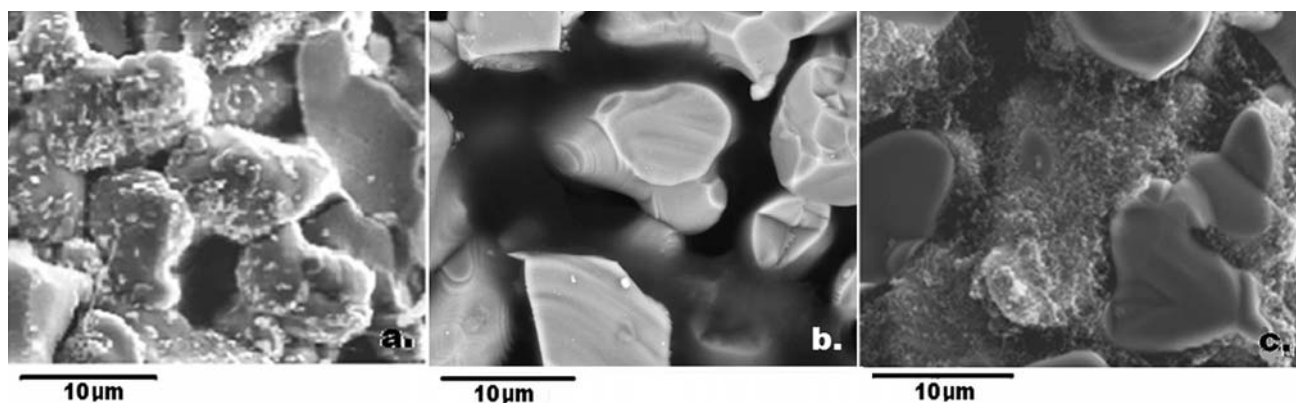
Figure 2. SEM imagines of TiO_2-ZrO_2 tubular ceramic (a), RF-xerogel/TiO_2-ZrO_2 (b), and C-xerogel/TiO_2-ZrO_2 (c).
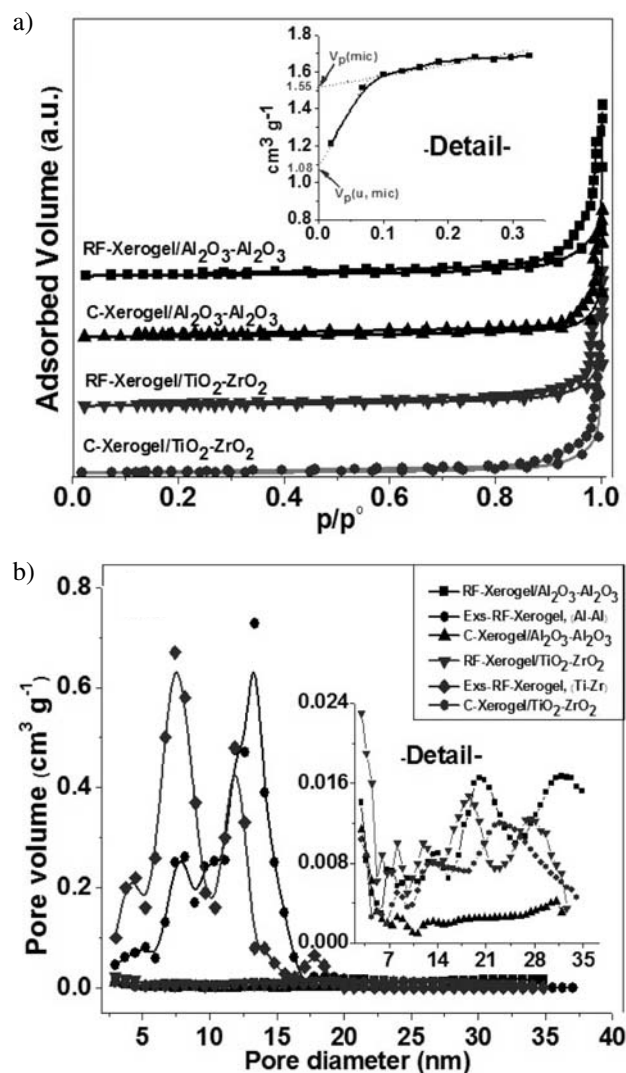
a)

b)

Figure 3. Adsorption-desorption isotherms of xeogel/ceramic composites (a) and pore size distribution of prepared xerogel/ceramic membranes and isolated RF-xerogels performed by BJH method (b).

condensation is absent (or only detectable at high *p/p°*).[25] In the Detail of Figure 3a adsorption isotherm of RF-xero-gel/αAl_2O_3-γAl_2O_3 at *p/p°* < 0.4 is presented. The isotherms of the other xerogel/ceramic composites are similar. The low slope signifies that multilayer adsorption has occurred on a relatively small external surface. By using of back-extrapolations of the linear section of isotherms at *p/p°* = 0.1–0.4 and *p/p°* < 0.05 at the intercept on the adsorbed volume axis (*p/p°* = 0.0) the *total effective micropore volume* v_p(mic) and *effective ultramicropore volume* v_p(u,mic), respectively, were obtained (Detail of Figure 3a).[26] The values of these effective micropore and ultramicropore volumes were higher than those estimated by HK method (Table 1). Additional evaluation about ultramicroporosity of obtained materials was revealed by gas permeation investigation (see Section 3.2).

In the Detail of Figure 3b an increase trend for pore volume with diameters < 5 nm is showed. Also, a decrease of BET surface area, meso- and micropore cumulative pore volumes and pore surfaces were obtained by pyrolysis of composite membranes (Table 1). In the case of xerogels/αAl_2O_3-γAl_2O_3, after pyrolytic step, an increase of cumulative mesopore surface was evidenced.
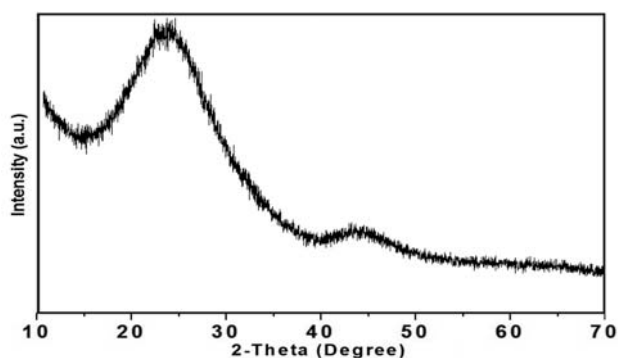

Figure 4. XRD pattern of Exs-RF-xerogel obtained outside of αAl_2O_3-γAl_2O_3 ceramic wall.

In order to identify the crystalline structure of the RF-and C-xerogels (the active part of the obtained membrane composites), X-ray diffraction analysis was perfor-

Table 1. Structural parameters of the prepared xerogel/ceramic composite membranes and the Exs-RF-xerogels determined by investigation of the N_2 adsorption-desorption isotherms.

SAMPLES	Mesopores**			Micropores**			
	S_{BET} [m^{2}g^{-1}] ± 0.1	S_{BJH} [m^{2}g^{-1}] ± 0.1	V_{BJH} x10^2 [cm^{3}g^{-1}]	S_{HK} [m^{2}g^{-1}] ± 0.1	V_{HK} x10^3 [cm^{3}g^{-1}]	V_p(mic) [cm^{3}g^{-1}] ± 0.01	V_p(u,mic) [cm^{3}g^{-1}] ± 0.01
RF-xerogel/Al$_2$O$_3$-Al$_2$O$_3$	4.8	5.1	1.1	4.4	2.6	1.55	1.08
Exs-RF-xerogel,(Al-Al)*	325	278	9.5	343	169.5	73	14.1
C-xerogel/Al$_2$O$_3$-Al$_2$O$_3$	4.1	5.9	0.3	3.7	2.2	1.16	1.10
RF-xerogel/TiO$_2$-ZrO$_2$	5.3	8.9	1.0	4.2	2.7	1.22	0.72
Exs-RF-xerogel,(Ti-Zr)*	317	341	11.2	310	164.2	69	34.3
C-xerogel/TiO$_2$-ZrO$_2$	3.7	3.7	0.7	3.7	2.0	1.31	1.09

*RF-xerogel excess of RF-xerogel/αAl_2O_3-γAl_2O_3 and RF-xerogel/TiO$_2$-ZrO$_2$, respectively; **S_{BJH}, V_{BJH}, S_{HK} and V_{HK} – surface area and pore volume determinate by Barrett–Joyner–Halenda method and Horvath-Kawazoe, respectively; V_p(mic) – effective micropore volume and V_p(u,mic) – effective ultramicropore volume.

Acta Chim. Slov. **2013**, 60, (2), 343–350

347

med for the excess of RF-and C-xerogels (collected from the outside of the composite walls). The XRD pattern of the Exs-RF-xerogel presented in Figure 4, shows two large peaks located at about $2\theta = 24°$ and $44°$ which are specifically for an amorphous structure. Normally, these xerogels have the same structure as those placed into ceramic pores of the composites.

3. 2. Gas Permeation Investigation

For gas separation applications the minimum pore diameter of the xerogel/ceramic composite membranes must be in the magnitude order of gas molecular diameters. This means that it should be in ultramicropore realm.[13,19] By performing the sol-gel process inside of porous ceramic walls a decrease of pore diameter, from macro-meso to meso-micropore succeeded (Figure 3, Table 1). Also, to be suitable for gas separation the xerogel should have open pore structure (Figure 5a), not closed one (Figure 5b). By crossing interest gases at various trans-membrane pressures through walls of composite membranes an open ultramicropore structure was confirmed as minimum pore diameter for obtained materials.
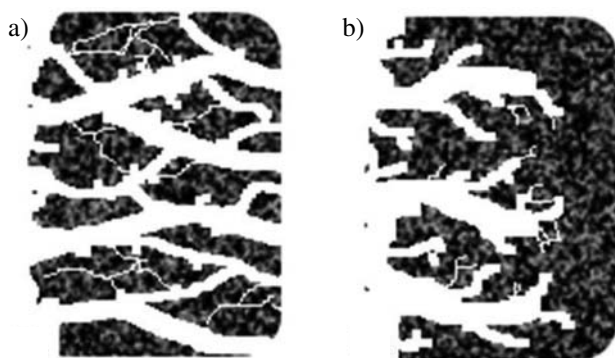

Figure 5. Open pore (a) and closed pore (b) structure materials.

The gas permeance (Q), expressed in GPU (GPU = 10^{-6} cm^3 (STP)/(cm^2 · s · cm$_{Hg}$)),[10] was used to quantify gas permeation trough obtained composite membranes. This was determinate by using the relation:

$$Q = \frac{F_{gas}}{2\pi rL} \cdot \frac{1}{\Delta p}, \qquad (1)$$

where F_{gas} is the cross-membrane gas flow (ml min^{-1}), r the ceramic tube radius (cm), L the active permeation length of tubular membrane (cm) and Δp the trans-membrane pressure (bar or 75 cm$_{Hg}$). The ideal selectivity of the membrane was defined as the ratio of H_2 permeance to the permeance of the other gases, measured at the same working parameters: trans-membrane pressure, temperature, ratio between interest gas and Ar flows.

A decrease of H_2 single gas permeances through RF-xerogel/αAl$_2$O$_3$-γAl$_2$O$_3$ membrane by trans-membra-

ne pressures increasing is showed in Figure 6. Quite constant values of H_2 permeance at various ratios between H_2 and Ar flows at the same trans-membrane pressure are noted.

In Figure 7, a decrease of gas permeance for RF-xerogel/αAl$_2$O$_3$-γAl$_2$O$_3$ membrane in rank $H_2 > CH_4 > CO > CO_2$, with a good fit to linear regression (R^2 = 0.9937–0.9968) respecting the Knudsen diffusion mechanism, is observed.[5]

It is known that the gas transport mechanism through molecular membranes depends on pore diameter and length. In the case of viscous flow mechanism, the gas permeation depends directly proportional to trans-membrane pressure. Therefore, in obtained composite mem-
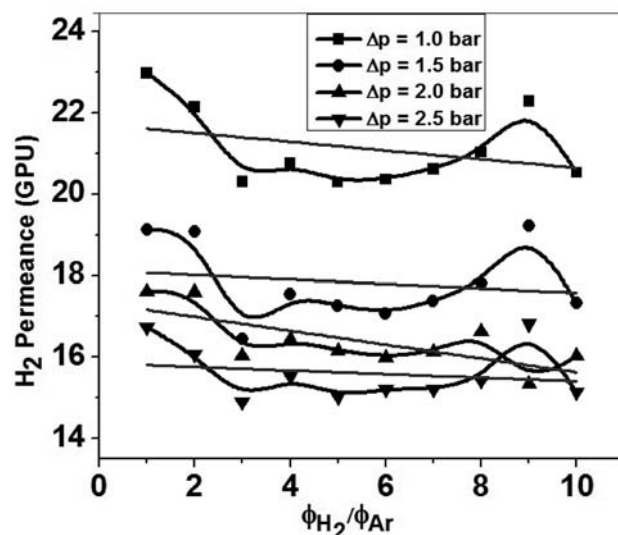

Figure 6. H_2 permeance through RF-xerogel/αAl$_2$O$_3$-γAl$_2$O$_3$ membrane at various trans-membrane pressure (p) and ratio between H_2 (Φ_{H2}) and Ar (Φ_{Ar}) flows.
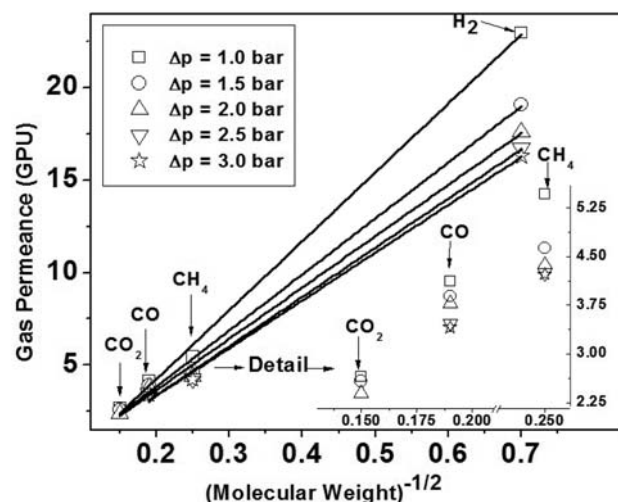
Figure 7. Gas permeances *vs.* (molecular weight)$^{-1/2}$ for RF-xerogel/αAl$_2$O$_3$-γAl$_2$O$_3$ membrane at different trans-membrane pressures and various ratios of interest gases (Φ_{Gas}) and Ar (Φ_{Ar}) flows.

348

Acta Chim. Slov. **2013**, *60*, (2), 343–350

branes, viscous flow is not considered predominant transport mechanism.[10,27]

An addition, as it is observed in Figure 7, the permeance varies with the inverse of the square root of the molar mass of the gas, which suggests the existence of Knudsen diffusion transport mechanism. But, higher H_2/gas ideal selectivity values than Knudsen selectivity values (Figure 8) show the presence of surface diffusion mechanism into RF-xerogel/αAl_2O_3-γAl_2O_3. It means that the transport mechanism could be a combination between surface diffusion mechanism characteristic of microporous polymers[5,28] and Knudsen diffusion mechanism characteristic of meso-macroporous ceramics[13,24], and the polymer selectivity properties are dominant to the ceramic support influence.[5,28] This combination indicates a complex open pore tridimensional structure.

A comparison between RF-xerogel/αAl_2O_3-γAl_2O_3 and RF-xerogel/TiO_2-ZrO_2 membranes for the H_2 permeance performed at various trans-membrane pressures is presented in Figure 9. Hydrogen permeance values are higher in RF-xerogel/TiO_2-ZrO_2 compared with that obtained in RF-xerogel/αAl_2O_3-γAl_2O_3 may be due to difference between the thicknesses of the membrane given by walls' thicknesses.[5]

A decrease of gas separation activity for C-xerogel/ceramic composite membranes compared with RF-

ones was observed. More of this, only the C-xerogel/TiO_2-ZrO_2 composite membrane, obtained by pyrolytic process, presents permeation properties for H_2 and CH_4 at 1 bar trans-membrane pressure, but the value of the ideal selectivity is lower than Knudsen selectivity (Table 2).

The explanation could be the shrinkage of the xerogel during pyrolysis[20] which generates new gas-cross ways. Also, the thickness and composition of the ceramic supports could influence the formation of different pore populations.[13,29] The carbon structure obtained into αAl_2O_3-γAl_2O_3 does not allow gas separation, possible due to pinholes, defects and/or the lower thickness of the ceramic walls.

Reproducibility and stability (operating life) were verified by measuring (three times) H_2 permeation through RF-xerogel/αAl_2O_3-γAl_2O_3 and RF-xerogel/TiO_2-ZrO_2 composite membranes (the most performing). The calculated relative standard deviations (RSDs) for H_2 permeance and H_2/CH_4 ideal selectivity (at 1 atm trans-membrane pressure, 25 °C) through RF-xerogel/αAl_2O_3-γAl_2O_3 were 5.25% and 5.95% respectively. For RF-xerogel/TiO_2-ZrO_2 the corresponding values were 10.6% and 8.8%, respectively. These results prove the reproducibility and stability of the composite membranes. The synthesis protocol of the composite membranes does not involve scalability issues; possible problems could be related to
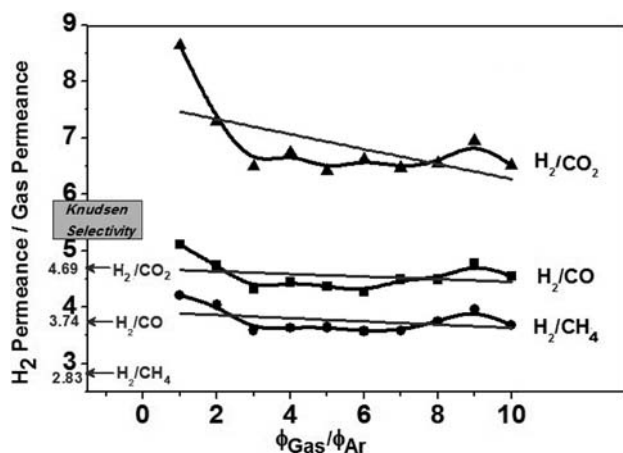

Figure 8. Ideal selectivity of H_2 and other gases of interest through RF-xerogel/αAl_2O_3-γAl_2O_3 membrane at 1 atm trans-membrane pressure and various gas (Φ_{Gas}) / Ar (Φ_{Ar}) flow ratios. Also, Knudsen selectivity for each H_2/Gas couples was exposed.
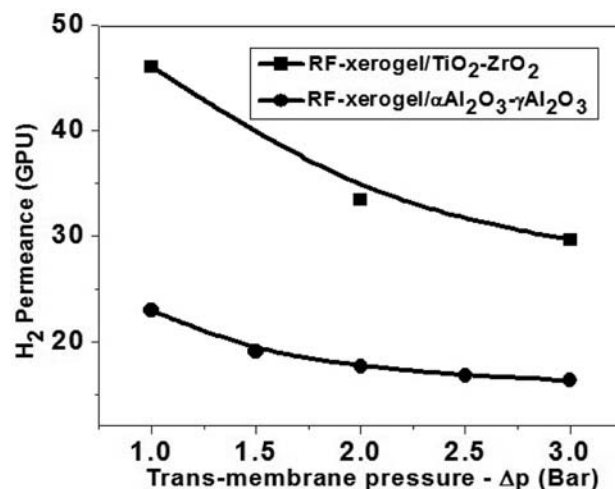

Figure 9. H_2 ideal selectivity through RF-xerogel/αAl_2O_3-γAl_2O_3 and RF-xerogel/TiO_2-ZrO_2 membranes at various trans-membrane pressures and the same value of H_2 and Ar flows.

Table 2. Permeance and ideal selectivity for H_2 and CH_4 through C-xerogel/ceramic membrane (trans-membrane pressure is 1 bar and gas/Ar flows is 1).

MEMBRANE	Trans-membrane Pressure (bar)	Permeance CH_4 (GPU)	Permeance H_2 (GPU)	Ideal Selectivity H_2/CH_4
C-xerogel/TiO_2-ZrO_2	1	436	989	2.27
C-xerogel/αAl_2O_3-γAl_2O_3		Not proper	Not proper	–
Knudsen Selectivity				2.83

Acta Chim. Slov. **2013**, *60*, (2), 343–350

349

Table 3. Permeance and ideal selectivity values of various membrane types.

		Permeance				Ideal Selectivity					***KS
		H_2 (GPU)	CH_4 (GPU)	N_2 (GPU)	He (GPU)	H_2/CH_4	H_2/CO	H_2/CO_2	He/N_2	H_2/N_2	
C-film/						10.6					2.83
TiO_2-ZrO_2[6]	*C						4.7				3.74
								2.37			4.69
6FDA-MDA[30]	*C			2.9	125.3				43.2		2.65
TBH-FPC[30]	*C			364	473				1.2		2.65
PEI[31]	**HF	16		0.32						50	3.74
RF-xerogel/		23.1	5.3			4.35					2.83
Al_2O_3-Al_2O_3	*C						5.2				3.74
								8.6			4.69
RF-xerogel/	*C	45.5	5.5			8.27					2.83
TiO_2-ZrO_2											

*C = composite; **HF = Hollow-Fiber; ***KS = Knudsen Selectivity.

the requirements of the targeted application (e.g. reactor dimensions), the size of the commercial ceramic supports (αAl_2O_3-γAl_2O_3 and TiO_2-ZrO_2 tubes are provided by the producers with a maximum length), etc.

Comparing the values of the ideal composite membranes and Knudsen selectivity of the other membrane types[6,30,31] it can be concluded that the obtained RF-xerogel/ceramic membranes are promising for separation of small gases (Table 3).

C-xerogel/ceramic membranes resulted by polymer/ceramic membrane pyrolysis could be suitable for gases with larger molecular size as those from petroleum industry. These composite membranes are also promising from the fabrication point of view. However, these results are preliminary.

4. Conclusions

Very stable and with controlled morpho-structural characteristics ultramicroporous RF- and C-xerogels/porous tubular ceramic (TiO_2-ZrO_2 and αAl_2O_3-γAl_2O_3) composite membranes were prepared. From the best of our knowledge is the first time when the synthesis of these composite membranes is reported and they were tested in gas separation applications.

The gas (H_2, CH_4, CO_2 and CO) permeation investigation indicated that the structure of the obtained RF- and C-xerogel/ceramic composites is formed by open-interconnected ultramicropores that permit gas diffusion and separation. The gas permeations using RF-xerogel/ceramic membranes are pressure and molecular mass dependent. From all synthesized xerogel/ceramic membranes, RF-xerogel/TiO_2-ZrO_2 presents the best activity for H_2 permeation (45.5 GPU at 1 bar of trans-membrane pressure and 25 °C). However, the additional research has to be carried out in order to optimize pore size tailoring.

6. References

1. D. Chensong, *J. Composite Mat.,* **2009**, *43(22),* 2639–2652.
2. U. Thanganathan, M. Nogami, *J. Non-Cryst. Solids,* **2010**, *356* 2799–2802.
3. M. E. Hossain, *J. Composite Mat.,* **2011**, *45(20),* 2133–2144.
4. X. Yin, J. Wang, N. Chu, J. Yang, J. Lu, Y. Zhang, D. Yin, *J. Membr. Sci,.* **2010**, *348,* 181–189.
5. K. Briceño, A. Iulianelli, D. Montané, R. Garcia-Valls, A. Basile, *Int. J. Hydrogen Energ.,* **2012**, 13536–13544.
6. K. Briceño, D. Montané, R. Garcia-Valls, A. Iulianelli, A. Basile, *J. Membr. Sci.,* **2012**, *415–416,* 288–297.
7. B. T. Carbon, **2011,** *49,* 2104–2112.
8. P. S. Tin, H. Y. Lin, R. C. Ong, T.-S., Chung, *Carbon,* **2011**, *49,* 369–375.
9. S. H. Han, G. W. Kim, C. H. Jung, Y. M. Lee, *Desalination,* **2008**, *233,* 88–95.
10. D. Montané, K. Briceño, R. Garcia-Valls, in: D. Stolten, T. Grube (Eds.), Parallel Sessions Book 3: Hydrogen Production Technologies - Part 2, *18th – WHEC,* 78–3, **2010**, Essen, pp. 466–473.
11. K.M. Steel, W. J. Koros, *Carbon,* **2003**, *41,* 253–266.
12. C. M. Veziri, G. N. Karanikolos, G. Pilatos, E. C. Vermiso-

glou, K. Giannakopoulos, Ch. Stogios, N. K. Kanellopoulos, *Carbon,* **2009,** *47,* 2161–2173.

13. A. F. Ismail, K. Li, in: R. Mallada, M. Menendez, (Eds.), *Membr. Sci. Tech. Series*, 13**,** Elsever, Oxford, **2008,** pp. 81–119.

14. W. Wei, G. Qin, H. Hu, L You, G. Chen, *J. Membr. Sci.,* **2007,** *303,* 80–85.

15. X. Zhang, H. Hu, Y. Zhu, S. Zhu, *J. Membr. Sci.*, **2007,** *289,* 86–91.

16. S. M. Chathoth, E. Mamontov, Y. B. Melnichenko, M. Zamponi, *Microp. Mesop. Mat.*, **2010,** *132,* 148–153.

17. L. M. Marques, F. L. Conceição, M. M. L. Ribeiro Carrott, P. J. M. Carrott, *Fuel Proces. Tech.,* **2011,** *92,* 229–233.

15. H. Ku, F. Cardona, N. Pattarachaiyakoop, M. Trada, *J. Composite Mat.*, **2009,** *43(7),* 741–754.

19. M. Inagaki, *New Carbon Materials*, **2009,** *24(3),* 193–232.

20. L. C. Cotet, A. Roig, I. C. Popescu, V. Cosoveanu, E. Molins, V. Danciu, *Rev. Roum. Chim.,* **2007,** *52(11),* 1077–1081.

21. L. Zubizarreta, A. Arenillas, A. Domínguez, J. A. Menéndez, J. J. Pis, *J. Non-Cryst. Solids*, **2008,** *354,* 817–825.

22. X. Wang, X. Wang, L. Liu, L. Bai, H. An, L. Zheng, L. Yi, *J. Non-Cryst. Solids,* **2011,** *357,* 793–797.

23. A. Maicaneanu, L. C. Cotet, V. Danciu, M., Stanca, *Stud. U. Babes-Bol. Che.,* **2009,** *54(4),* 33–42.

24. D. Lee, L. Zhang, S. T. Oyama, S. Niu, R. F. Saraf, *J. Membr. Sci.,* **2004,** *231,* 117–126.

25. F. Rouquerol, F. Rouquerol, K. Sing, in: Academic Press (Ed.): Adsorption by Powders and Solids, Principles Methodology and Applicationa, San Diego, USA, **1999,** pp. 219–281.

26. E. Maglara, A. Pullen, D. Sulivan, W.C. Conner, *Langmuir*, **1994,** *10,* 4167–4173.

27. C. Yacou, A. Ayral, A. Giroir-Fendler, M. L. Fontaine, A. Julbe, *Microp. Mesop. Mat.,* **2009,** *126,* 222–227.

28. M. Saeidi, M. T. Moghadam, M. Mahdyarfar, T. Mohammadi, *Asia-Pac. J. Chem. Eng.,* **2010,** *5,* 324–329.

29. H. Kawakami, M. Mikawa, S. Nagaoka, *J. Membr, Sci.,* **1997,** *137,* 241–250.

30. M. E. Rezac, W. J. Koros, *J. App. Poly. Sci.,* **1992,** *46,* 1327–1338.

31. D. Wang, W.K. Teo, K. Li, *J. App. Poly. Sci.,* **2002,** *86,* 698–702.

Povzetek

Nove, zelo stabilne kompozite, smo pripravili z nanosom resorcinol-formaldehidnega (RF-) polimera ali ogljikovega (C-) kserogela na stene komercialnih poroznih keramičnih cevnih elementov (TiO_2-ZrO_2 in αAl_2O_3-γAl_2O_3). Materiali so bili pripravljeni s sol gel postopkom, ki mu je sledilo sušenje in piroliza (le v primeru C-kserogel kompozitov). Materiale smo karakterizirali z absorbcijo-desorbcijo dušika, vrstično elektronsko mikroskopijo in rentgensko praškovno analizo ter testirali za morebitno uporabo pri separaciji plinov (H_2, CH_4, CO_2 in CO). Dodatne morfološke in strukturne informacije o odprti ultramikroporozni strukturi smo pridobili z meritvami prepustnosti izbranih plinov. Zanimivi so bili predvsem rezultati meritev prepustnosti H_2, še posebej v primeru RF- kompozitov ob upoštevanju mehanizma Knudsenove difuzije za prepustnosti plinov: $H_2 > CH_4 > CO > CO_2$. Potrdili smo sočasen obstoj mehanizmov Knudsenove in površinske difuzije.